Journal of King Saud University – Science 33 (2021) 101597

Contents lists available at ScienceDirect

Journal of King Saud University – Science

journal homepage: www.sciencedirect.com

Original article

Conversion of glycerol to hydroxyacetone over $SrTiO_3$ -type perovskite: A DFT study

Ignacio Lizana [a,b,1], Julio Colmenares-Zerpa [a,c,1], Gina Pecchi [a,b], R.J. Chimentão [a,*], Eduardo J. Delgado [a,b,*]

[a] Physical Chemistry Department, Faculty of Chemical Sciences, University of Concepcion, Casilla 160-C, Concepción, Chile
[b] Millennium Nucleus on Catalytic Processes Towards Sustainable Chemistry, Santiago 4070386, Chile
[c] Laboratory of Kinetics and Catalysis, Department of Chemistry, Faculty of Sciences, University of Los Andes, Mérida 5101, Venezuela

ARTICLE INFO

Article history:
Received 25 January 2021
Revised 5 June 2021
Accepted 31 August 2021
Available online 9 September 2021

Keywords:
DFT
Glycerol
Dehydration
Hydroxyacetone
Perovskite
Mechanism

ABSTRACT

Glycerol is currently a co-product of biodiesel production, and it is well-known to be a platform molecule, which is widely used in etherification, dehydration, dehydrogenation, oxidation, and reforming reactions, to produce chemicals of high value for the chemical industry. In this study, we theoretically address the dehydration of glycerol over the $SrTiO_3$-type perovskite. The study includes the characterization of the transition states and intermediates occurring along the reaction pathway, and a possible mechanism is proposed, as well. The results show that the dehydration of glycerol occurs via a four-stage mechanism corresponding to the adsorption of glycerol on the perovskite, the surface reaction to produce the adsorbed dihydroxyacetone, the elimination of water produce 2,3-enol, and finally the desorption of this enol, which in turn undergoes keto-enol tautomeric equilibrium to form hydroxyacetone (HA). The rate-limiting stage corresponds to the formation of 2,3-enol showing an activation barrier of 106.3 kcal/mol.

1. Introduction

Biomass is an important strategy to produce chemicals and fuels, and as an alternative energy source due to both economic and environmental reasons. The catalytic transformation of biomass represents one of the most important processes to produce chemicals and biofuels. Among the most important biomass precursors, can be highlighted alcohols containing multiple hydroxyl groups such as ethylene glycol, 1,2- and 1,3-propanediol, and glycerol (Coma et al., 2017).

Glycerol is produced as a co-product of saponification of fats and in the transesterification of vegetable oils to biodiesel (Behr, 2008). From biodiesel production, glycerol is obtained in a ratio of 10% in mass of glycerol to biodiesel, and hence, increased biodiesel worldwide implies larger volumes of glycerol added to the market (Sels et al., 2007). The surplus of glycerol makes it remarkable and attractive as a platform molecule for the sustainable production of various value-added chemicals such as acrolein and hydroxyacetone (HA) by a dehydration reaction.

Heterogeneous catalytic processes for the selective transformation of glycerol are the preferred strategy because it allows the separation of the catalyst from the process and avoids waste disposal drawbacks (Célerier et al., 2018). Glycerol dehydration is usually performed over acid-basic solids catalysts in the liquid or gas phase using solid acid-base catalysts including sulfates, phosphates, and zeolites. Hydroxyacetone can be obtained from glycerol dehydration over catalysts containing Lewis acid sites such as MO_x-Al_2O_3-PO_4 (Suprun et al., 2011), Zn-Cr oxides (Alhanash et al., 2010) or catalysts containing basic sites such as $NiCo_2O_4$ (Lima et al., 2011).

The physical–chemical properties of the catalyst determine the route of glycerol dehydration. In presence of Brönsted acid sites (BAS) glycerol can suffer dehydration driving the chemical route to the production of 1,3-enol which produces 3-hydroxypropanal through a keto-enol tautomerization, and acrolein is finally produced by dehydration of the 3-hydroxypropanal. Regarding the Lewis acid sites (LAS), glycerol can suffer dehydration producing 2,3-enol, which is converted into HA by a keto-enol tautomeric equilibrium (Pompeo et al., 2010). Pompeo et al. (2010) reported a chemical route in which glycerol can firstly suffer either

---

* Corresponding authors at: Physical Chemistry Department, Faculty of Chemical Sciences, University of Concepción, Edmundo Larenas, 129, Casilla 160-C, Concepcion, Chile.

E-mail addresses: rchimenton@udec.cl (R.J. Chimentão), edelgado@udec.cl (E.J. Delgado).

[1] These authors contributed equally to this work.

Peer review under responsibility of King Saud University.

Production and hosting by Elsevier

https://doi.org/10.1016/j.jksus.2021.101597

dehydrogenation to form dihydroxyacetone or glyceraldehyde on the metallic sites. Once dihydroxyacetone is formed, it can be dehydrated followed by hydrogenation to generate HA. It has been also reported (Lari et al., 2015) that dihydroxyacetone can be dehydrated towards pyruvaldehyde over a combination of Brönsted and Lewis acid sites. On the other hand, glyceraldehyde can either dehydrate to produce 2-hydroxyacrolein or pyruvaldehyde and finally hydrogenated to produce HA. Based on the literature, the chemical route is illustrated in Scheme 1.

Previous reports argued that HA can be formed by: i) the coordination of the basic electrons of oxygen in the primary hydroxyl group of glycerol with the surface Lewis acid sites of the metal oxide and ii) an H atom in the secondary hydroxyl group of glycerol with a surface oxygen of the metal oxide (Kinage et al., 2010).

The role of the basic sites in the conversion of glycerol has been also reported by Célerier et al. (2018) who indicated that basic properties do not exert a net effect on the dehydration of glycerol in the gas phase towards HA on copper catalysts supported on MgF(OH) and MgO, whereas Stošić et al. (2014) indicated that basic metal oxides sites improve the yield towards HA. In this respect, it must be remarked that the selective dehydration of glycerol to HA could also occur over basic catalysts, starting with a dehydrogenation step and not with a dehydration step as proposed for acid catalysts.

The catalytic biomass-derived compounds transformation is often carried out in an aqueous medium. Because water molecules coordinate with the active Lewis acid sites, aqueous reaction medium generally entailed lower rates and lower yields (Dapsens et al., 2015). In addition, the leaching of active species deactivates the catalysts, contaminates the products, and increases the cost of product purification (Li et al., 2020). Therefore, demands to design a new generation of active catalysts to produce selectively HA under mild conditions and aqueous environment in the glycerol dehydration is still a challenger.

Mixed-metal oxides are usually investigated and industrially used as solid acid-base catalysts in the catalytic processes due to the accomplishment of stability requirements against leaching. Perovskites are mixed oxides of general formula ABO_3, wherein A represents a lanthanide metal, alkali metal, or alkaline earth metal, and B a lanthanide metal. These compounds show high oxygen mobility, extraordinary tolerance for metal substitutions in the lattice structure, high thermal stability, and also resistance to sintering (Polo-Garzon and Wu, 2018). On the other hand, the partial substitution, doping, of the metals allow the stabilization of uncommon oxidation states, along with the simultaneous formation of oxygen vacancies in the crystal lattice (Pecchi et al., 2011). It must also be added that the possibility of the combination of different metals can greatly improve the catalytic performance of mixed-metal oxides (Arandiyan and Parvari, 2009). Perovskite structure can tolerate substitutions in one or both cationic sites (A and B sites) while preserving their original crystal structure. The preparation of perovskite entails a simple chemical method, and its industrialization requires a low-cost implementation.

To rationalize the design of efficient catalytic systems for the transformation of derived compounds from biomass such as glycerol, it is relevant an in-depth understanding of the surface interactions of reactive molecules with the acid and basic sites of metal oxides. Previous work dealing with DFT calculation reported that glycerol formed bridging alkoxy bond through a primary alcohol group to metal atoms of the metal oxide surface and an additional surface interaction via hydrogen-bonding between its secondary alcohol group and the basic surface oxygen atom of the metal oxide (Copeland et al., 2013a). Hydroxyl groups of the glycerol molecule are usually designated as terminals for positions 1 and 3 of the alkyl chain and central carbon for position 2. Even though glycerol reveals several stable conformations on metal surfaces (Chelli et al., 2000), it has been reported that the most stable conformation of glycerol on the Rh(1 1 1) surface shows two oxygens adsorbed atop sites of Rh and one hydrogen bond from the adsorbed terminal hydroxyl group to the other terminal hydroxyl. This conformation showed adsorption energy of −13.86 kcal/mol (Yang et al., 2007).

Reports on perovskite-catalyzed organic reaction for application in green chemistry have been limited so far. The knowledge of intermediates formed in the interaction of biomass molecules on metal oxide surfaces is of clear relevance to the development of

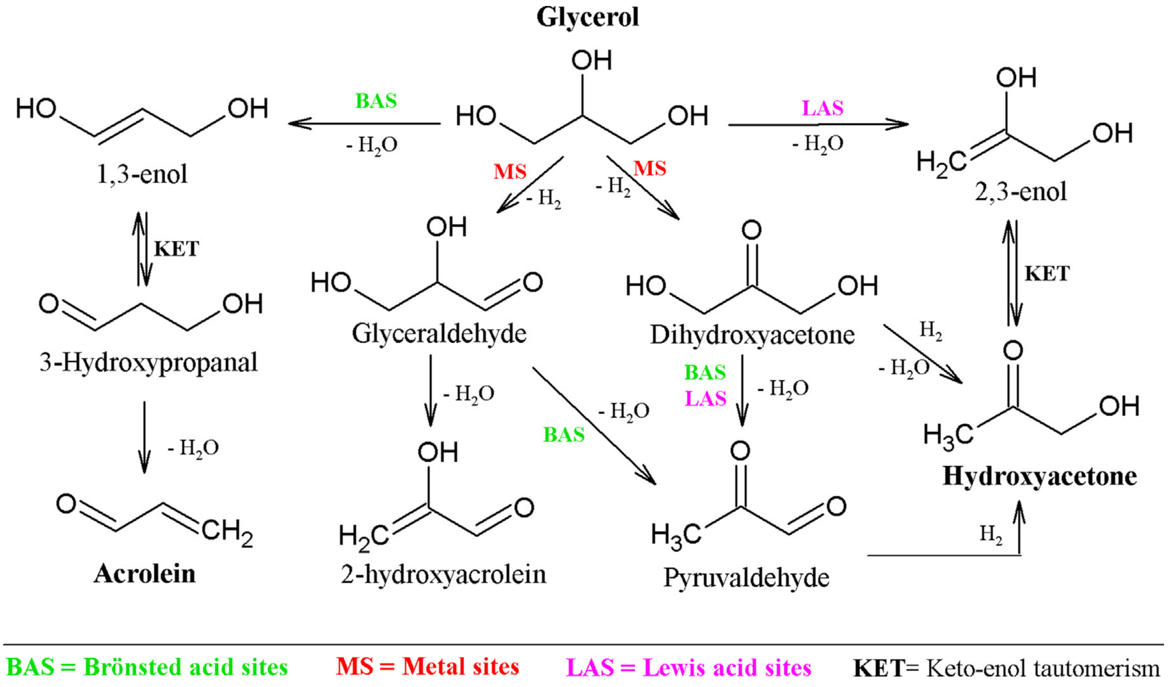

Scheme 1. Proposed general routes for HA and acrolein formation from glycerol conversion. Adapted from references (Lari et al., 2015; Pompeo et al., 2010).

heterogeneous catalyzed reactions. These issues have motivated the current study on glycerol dehydration to HA over $SrTiO_3$ perovskite, an extensively investigated perovskite with enhanced optical, electrical, and chemical properties. Perovskites have already proved to be selective to C-O cleavage and poorly active to C-C bond breaking (Polo-Garzon and Wu, 2018) and no report dealing with the dehydration of glycerol over perovskite-type oxides has been addressed neither experimental nor theoretical, so far.

To fill this gap, in this article for the first time we report the dehydration of glycerol over the $SrTiO_3$ perovskite from a theoretical point of view by a cluster model approach. Several studies using this methodology have been reported in the literature for the study of adsorption of gases on solids (Charoenwiangnuea et al., 2016; Housaindokht and Zamand, 2015) in order to evaluate energy barriers and to hypothesize possible dehydration mechanisms, as well. This study postulates that the combination of Lewis and Brönsted acid-base sites in the surface favors the proton exchange between surface and the adsorbate allowing in this way the selective dehydration of glycerol and consequently the selective formation of hydroxyacetone. The research aims to improve our understanding of the involved mechanism and its relationship with the surface properties as well.

2. Methodology calculations

The unit cell of the cubic $SrTiO_3$ perovskite (space group 221, $Pm\overline{3}m$, cell constant a = 3.90 Å (Longo et al., 2008)) was used to build the model. The super cell of dimensions (4 × 3 × 1), containing 60 atoms, was created by replication and expansion of the unit cell, involving a surface area of about 13.7 × 9.8 $Å^2$. The number of atoms considered in the super cell was chosen to have in mind the compromise between the computational cost and accuracy. The optimized structure is shown in Fig. 1. The interatomic distances for the Ti-O and Sr-O bonds are 1.95 and 2.76 Å, respectively. The calculated lattice constant a_0 of 3.86 Å is in good agreement with the experimental value reported above.

All calculations were carried out with Jaguar (Bochevarov et al., 2013), using the DFT framework within the molecular cluster approach. We choose the hybrid functional B3LYP and the LAV1S basis set for the calculations (Hay and Wadt, 1985). The convergence criteria used in the optimization was 10^{-6} Ha, as implemented in Jaguar. We use the natural bond orbital (NBO) population scheme for molecular orbital analysis and atomic charge calculations (Wadt and Hay, 1985). Finally, only the Ti-O terminated surface was considered in this study since, according to the literature, the A-sites of the perovskite are catalytically inactive (Carlotto et al., 2015).

To obtain the most stable configuration of glycerol adsorbed on the perovskite, we initially place the glycerol molecule over the surface at distance of 2.8 Å as shown in Fig. 2. Afterward, the systems were subject to geometry optimizations. In these minimizations, the surface atoms were kept fixed, while the atoms of the glycerol molecule were considered without any constraint. The energy of adsorption was calculated by means of the following equation:

$$E_{adsorption} = E_{complex} - \left(E_{SrTiO_3} + E_{glycerol}\right)_{isolated}$$

3. Results and discussion

3.1. Conformational space of glycerol

The conformation of glycerol has been widely investigated in gas (Chaminand et al., 2004), liquid (Shen et al., 2010), and solid states (Ketchie et al., 2007). It has been reported six backbone conformations are designed by the dihedral angles involving the carbon and oxygen atoms (Madura and Ul-Haq, 2017). It is proposed that there are 126 glycerol conformers which were characterized by computational analysis using different theory levels (Callam et al., 2001). Thus, the free glycerol molecule may exist in several isomeric forms according to the rotation of the dihedral angles α and β, O_1-C_1-C_2-O_2 and O_2-C_2-C_3-O_3, defined in Fig. 3. This is necessary to do to perform a conformational analysis to determine all local minima in the conformational space. To do this we explored the potential energy surface (PES) in terms of these two angles, with steps of 10°. The results show 9 local minima in the three- and two-dimensional representation of the PES (Fig. 4), and whose structures are shown in Fig. 5.

The minima are shown in Fig. 4(b). In this Figure, the global minimum is labeled with the letter (a), while the local minima are labeled with the letters going from (b) to (i). The energies reported are relatives to the global minimum (a); the values suggest that the several conformational forms may exchange from one to another considering the low values of energy involved. However, the results herein reported are based on the global minimum structure of glycerol. The glycerol structure used as the starting point is depicted in Fig. 5(a).

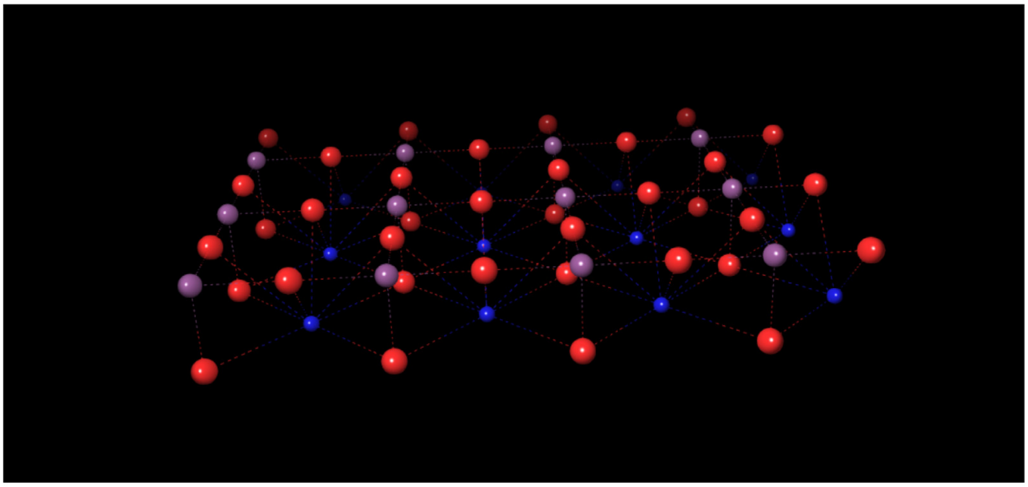

Fig. 1. Optimized structure of $SrTiO_3$ (red: oxygen atoms, blue: Sr atoms, purple: Ti atoms).

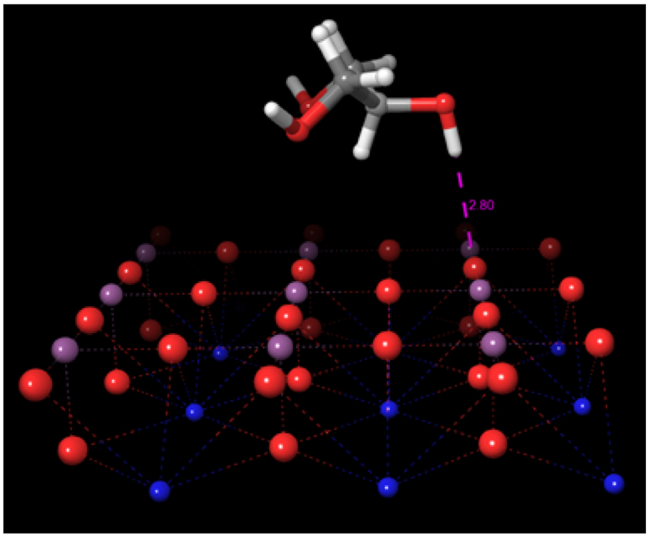

Fig. 2. Initial structure of the glycerol-perovskite complex.

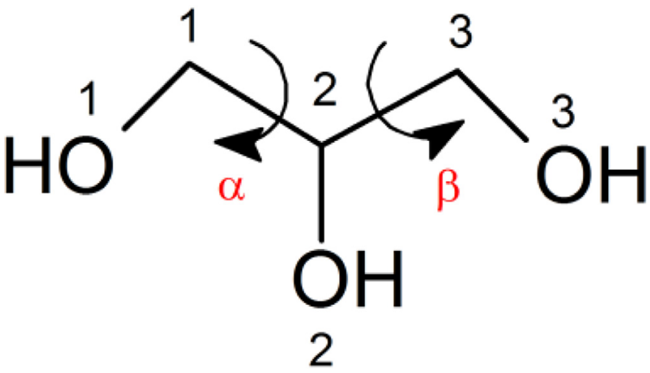

Fig. 3. Dihedral angles α and β defined in the glycerol molecule.

3.2. Adsorption of glycerol on the $SrTiO_3$ surface

Here, the investigation of the adsorption of glycerol on the $SrTiO_3$ surface considered only the Ti-O terminated surface. To model the phenomenon, we initially placed the glycerol molecule over the surface at a distance of 2.8 Å as shown in Fig. 2. Afterward, the system was subject to geometry optimizations. In these minimizations, the atoms of the perovskite were kept fixed, while the atoms of glycerol were considered without any constraint. The optimization procedure led to the glycerol-adsorbed complex shown in Fig. 6. In this optimized structure, it is observed that glycerol adsorbs in a non-dissociative or molecularly adsorbed way (Lewis-bound species) as expected for Lewis sites. The exposed surface of perovskites has the acidity and basicity attributed to the presence of cations ($M^{\delta+}$) and anions (O^{2-}) respectively. The acid strength of the sites is related to the effective positive charge of the surface whereas the effective negative charge and coordination on the surface are related to the basic strength of the surface sites (Polo-Garzon and Wu, 2018). The calculated energy of adsorption of glycerol on $SrTiO_3$ surface is -122.1 kcal/mol.

In this optimized structure, the hydroxyl hydrogen of the C_2 atom has a strong interaction with one oxygen of the lattice located at 1.47 Å, while the other two hydroxyl groups attached to the C_1 and C_3 atoms interact with two titanium atoms, acting as LAS, located at 2.12 and 2.13 Å, respectively. Additionally, there is an interaction between the hydrogen atom, attached to the C_2 atom, and an oxygen atom of the perovskite surface. Lewis acid sites are reported to be active sites for alkoxide bond formation from the adsorption of glycerol. Glycerol forms alkoxide surface species on metal oxides containing LAS. The additional surface interaction by the C_2 of glycerol is via a hydrogen bond of its secondary alcohol with a basic surface oxygen atom of the perovskite surface (Copeland et al., 2013b).

3.3. Surface reaction for the transformation of glycerol into dihydroxyacetone

Once glycerol is adsorbed over the surface, the reaction proceeds with the abstraction of the hydrogen atom attached to the C_2 atom by the interacting oxygen atom of the $SrTiO_3$ surface. It is noteworthy to mention that the one oxygen atom of the $SrTiO_3$ surface, acting as Brönsted base abstracts the proton from the C_2 atom of the adsorbed glycerol. This event enhances the acid

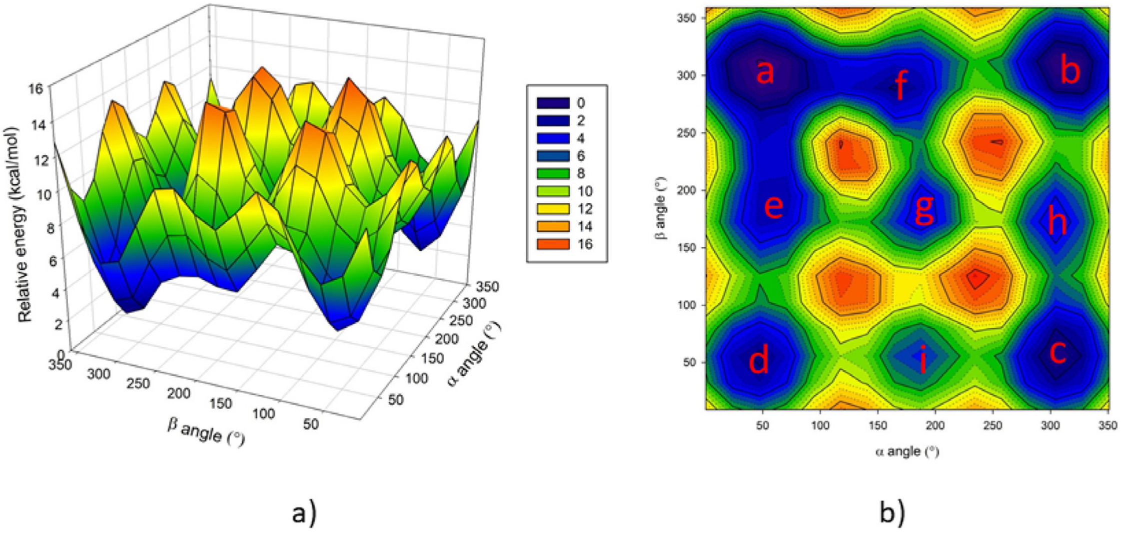

a) b)

Fig. 4. 3-D view (a), and 2-D view (b) of the potential energy surface.

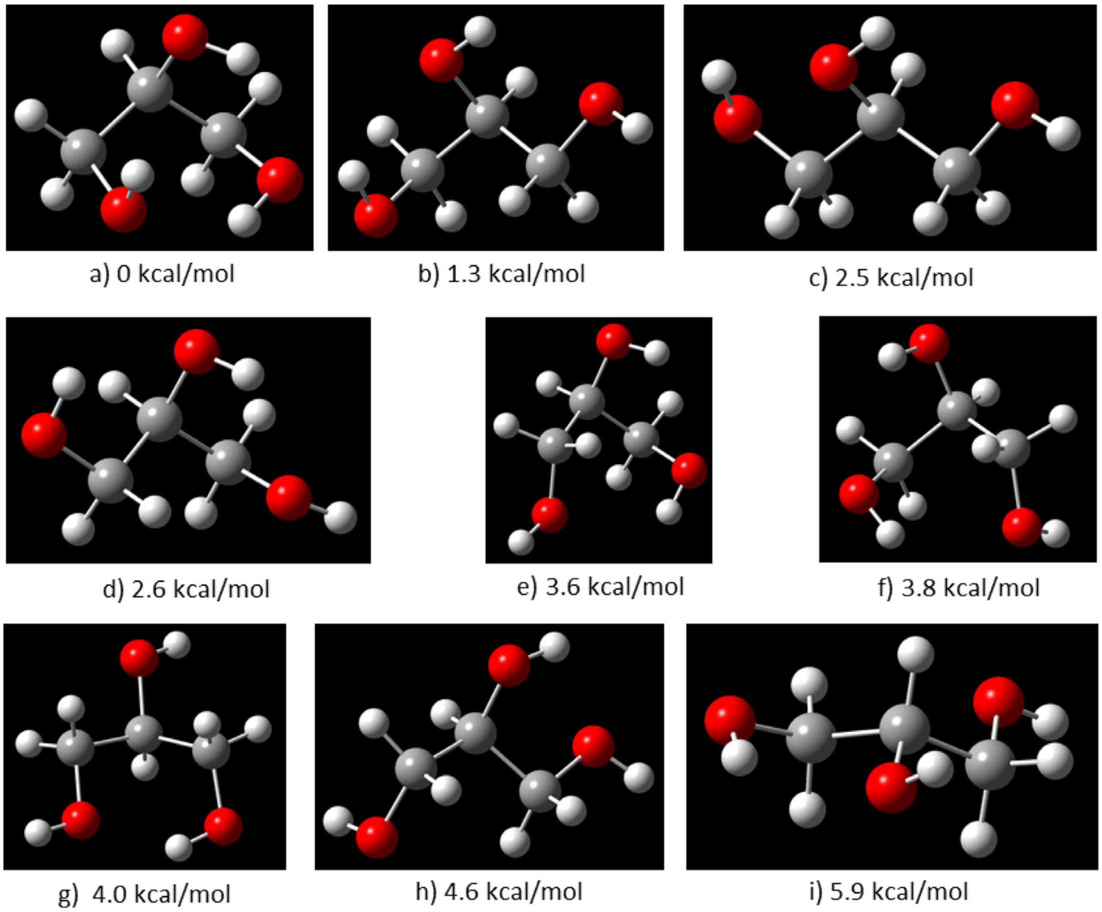
a) 0 kcal/mol
b) 1.3 kcal/mol
c) 2.5 kcal/mol
d) 2.6 kcal/mol
e) 3.6 kcal/mol
f) 3.8 kcal/mol
g) 4.0 kcal/mol
h) 4.6 kcal/mol
i) 5.9 kcal/mol

Fig. 5. Structures of glycerol corresponding to the minima observed in the PES and their corresponding energy relatives to the global minimum (red: oxygen atoms, white: hydrogen atoms, gray: carbon atoms).

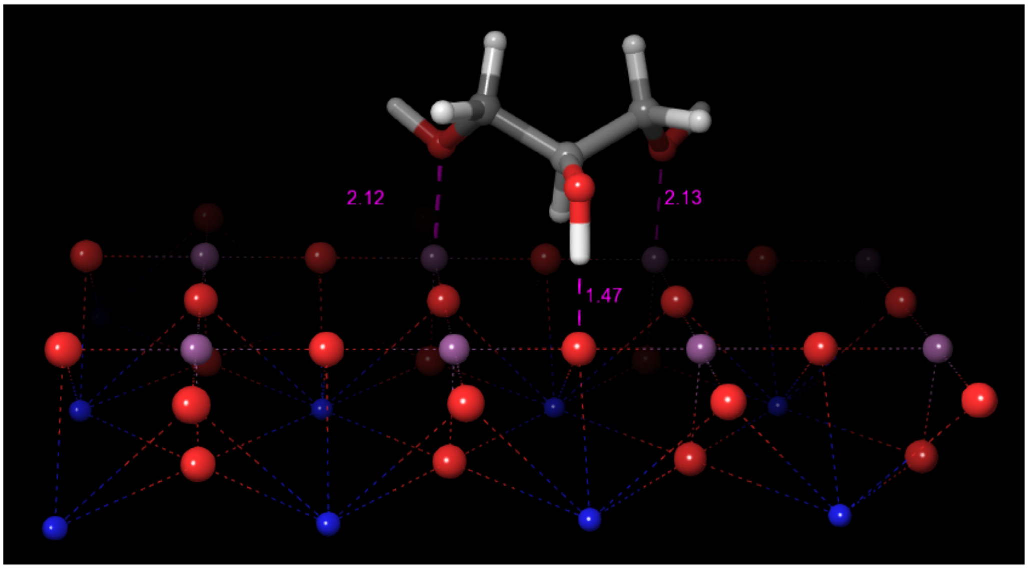

Fig. 6. Adsorbed glycerol on the $SrTiO_3$ surface.

character of C_2-hydroxyl group triggering its complete deprotonation forming the dihydroxyacetone. In these steps, the surface interacting oxygen atoms act as Brönsted bases, allowing in this way their protonation. Both transferences occur through a synchronous concerted mechanism via a transition state, TS-1, with a calculated activation barrier of 23.8 kcal/mol, and whose structure is shown in Fig. 7. The length of the C_2-O bond is 1.33 Å, while the bond angle O-C_2-C_1 is 117°; these figures account

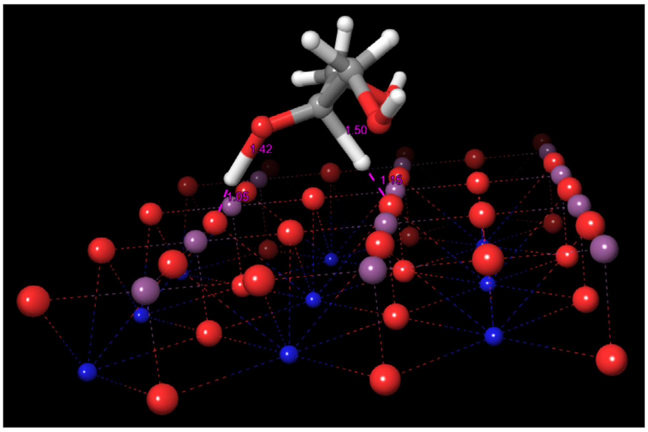

Fig. 7. Structure of the transition state TS-1.

for the transition of the C_2 atom from sp^3 hybridization to sp^2. The imaginary frequency has the value 816.6 cm^{-1} and the respective intensity is 3658, corresponding to the stretching of O-H and C-H bonds. A video of the imaginary frequencies associated with the transition state TS-1 can be viewed in the movie MV-1 in Supplementary Material.

The dihydroxyacetone molecule so formed is shown in Fig. 8. It is possible to observe the molecule over the surface, and the two hydrogen atoms attached to two oxygen atoms of the surface of the perovskite. Here, it is important to highlight that the selective dehydration reaction of glycerol to HA begins firstly with a dehydrogenation step on the secondary carbon of the glycerol molecule over the basic sites of the $SrTiO_3$ perovskite surface.

3.4. Formation of 2,3-enol and elimination of water

In the next stage of the mechanism, the resultant protonated oxygen atoms of the perovskite surface behave now as Brönsted acid sites, thus one of them protonates the carbonyl oxygen, while the other one protonates one of the hydroxyl oxygen of the formed dihydroxyacetone. The result of this step is the formation of 2,3-enol and the corresponding water elimination Fig. 9.

In the optimized structure shown, it can be observed the interactions of the oxygen of the eliminated water molecule with a titanium atom at 2.06 Å and the hydroxylic oxygen of the 2,3-enol linked to C_3 carbon frontally on another titanium atom over the surface at a distance of 2.17 Å. Also, an additional interaction is generated by the oxygen attached to the C_2 atom of the enol produced with an adjacent titanium atom at 2.26 Å. This event occurs in a concerted synchronous way via the occurrence of a transition state TS-2, whose structure is shown in Fig. 10. The structure of TS-2 shows a C-O bond length of 1.81 Å, and C_2 bond angles of about 115°, accounting for the water elimination and the change in the hybridization from sp^3 to sp^2 of the corresponding terminal carbon. The respective imaginary frequency has the value 774 cm^{-1} and intensity 2337, corresponding to the stretching of $O_{surface}$-H and C-O bonds. An animation of the imaginary frequency is shown in movie MV-2 of Supplementary Material. The calculated activation barrier for this step is 106.3 kcal/mol.

Based on previous research work of glycerol conversion on $CuCr_2O_4$ catalyst, the activation energy for the removal of a terminal hydroxyl group from adsorbed glycerol on Cu(1 1 1) was calculated to be 39.4 kcal/mol and on the other hand, the activation energy of 41.7 kcal/mol is required to cleavage the center hydroxyl group of glycerol (Yun et al., 2017). This suggests that the reaction pathway for C-O bond cleavage of a terminal hydroxyl group is kinetically more favorable than that of the center, which is also reasonable due to less steric hindrance. Thus, in light of the above-mentioned thermodynamic view, the path for hydroxyacetone generation via 2,3-enol seems to be preferable. This is exactly what we observed from our theoretical approach. In addition, it has been reported for glycerol dehydration with an H-ZSM-5 that the deprotonated hydroxyl oxygen species of the solid surface is recovered back from the secondary OH group from another adsorbed glycerol molecule by the secondary carbon C_2 which is closer to the deprotonated acid site of the H-ZSM-5 zeolite solid surface (Kongpatpanich et al., 2011).

3.5. Keto-enol tautomerism

Afterward, 2,3-enol desorbs to undergo keto-enol tautomerism mediated by water molecules to form HA, Fig. 11a, via the transition state TS-3, Fig. 11b. In this type of isomerization, which is characterized by the migration of a proton and the movement of a double bond described as the exchange of the π cloud between the C-C (in the enol) and C-O (in the ketone) bonds, the species corresponding to the keto tautomer rather than the enol species tend to be more stable (Wade, 2006). Generally, this can be roughly explained by the contribution of the characteristic

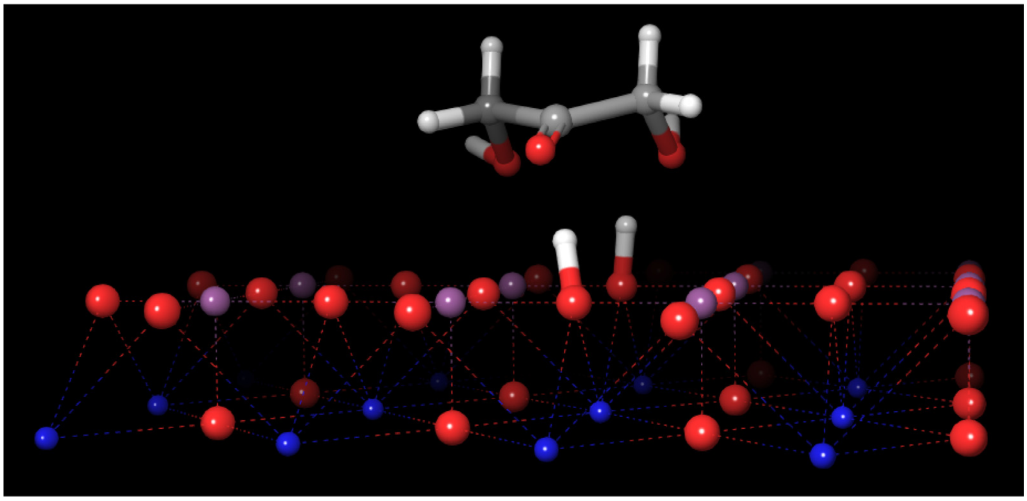

Fig. 8. Structure of the dihydroxyacetone-perovskite cluster.

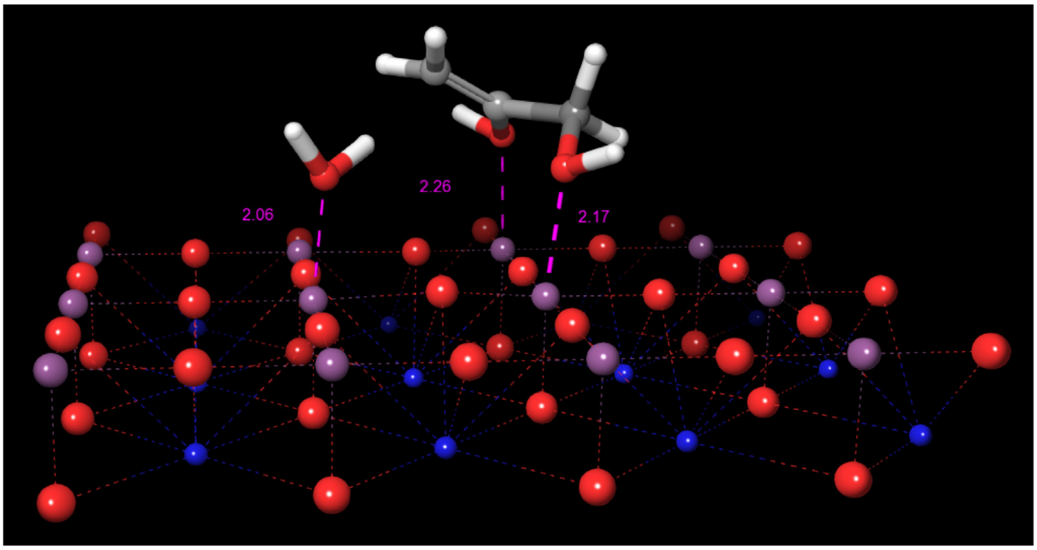

Fig. 9. Structure of the 2,3-enol-perovskite cluster.

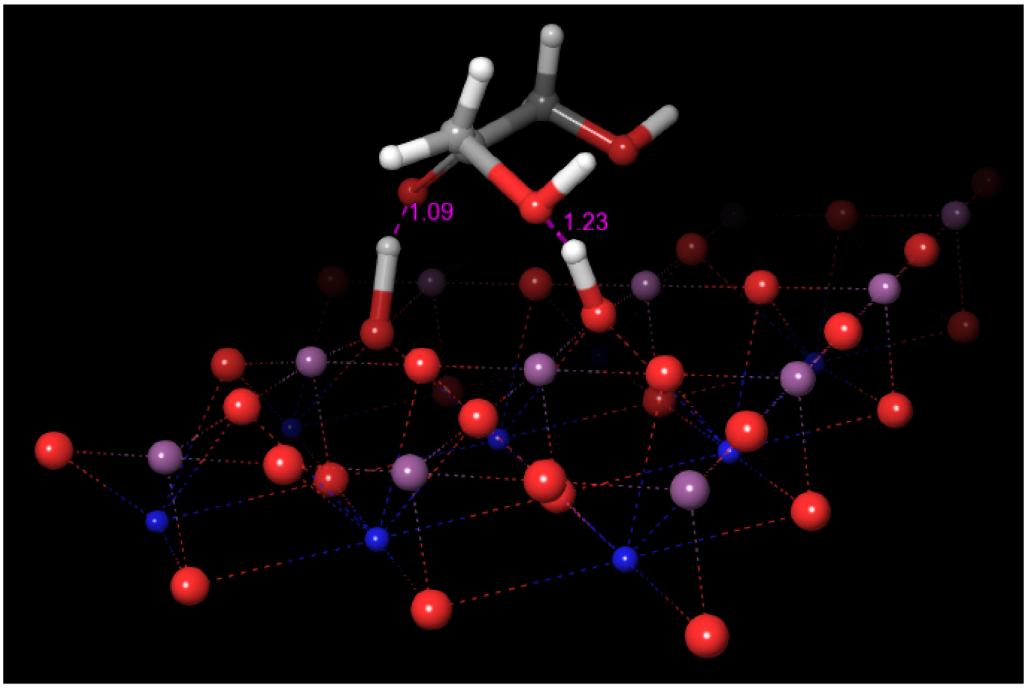

Fig. 10. Structure of the transition state TS-2.

bond energies in both types of tautomers; that is, the keto species has C-H, C-C, and C=O bonds with an approximate value of 359 kcal/mol, while the enol species consists of C=C, C-O, and O-H bonds with a value of 347 kcal/mol. This difference of 12 kcal/mol in the approximate total bond energy results in greater thermodynamic stability towards the keto tautomer (Smith and March, 2007). In addition to this, it is to be expected that in the absence of a conjugation effect (for example, due to the presence of α,β-unsaturated compounds) and of the absence of bulky-aryl- and fluorinated-groups directly attached to the enolic double bond, such as conditions of this work; the transformation of 2,3-enol into HA is highly favored (Smith and March, 2007).

An additional consideration to take into account is the keto-enol tautomerism related to the fact that this elementary reaction is recognized to be exergonic ($\Delta G_{\text{reaction},533\ K}$ = -14.4 kcal/mol) (Sanchez et al., 2019) and it is therefore expected to be spontaneous. In this respect, once the enol intermediate (2,3-enol) is generated, it is promptly transformed into HA. Another important issue to be emphasized for the occurrence of the keto-enol tautomerism is correlated to the presence of Lewis acid-base pairs as active sites on the surface of $SrTiO_3$-type perovskite which may decrease the energy barrier. The activation barrier for this stage is 47.6 kcal/mol. Previous work (Sanchez et al., 2019) focused on the investigation of glycerol dehydration over La_2CuO_4-type perovskite reported an activation value of 52.3 kcal/mol for the

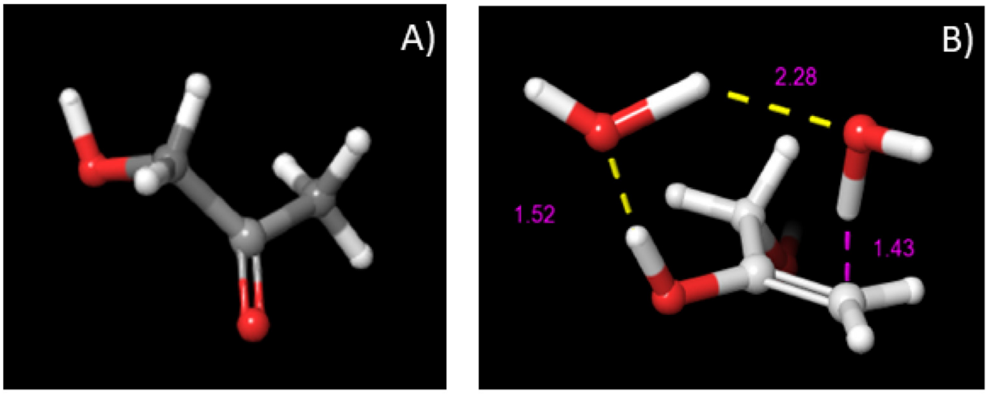

Fig. 11. Structure of hydroxyacetone (A); structure of the transition state TS-3 (B).

keto-enol tautomerism step which are in close agreement with our results. An animation of the involved imaginary frequency can be viewed in the movie MV-3 of Supplementary Material.

3.6. Overall energy diagram

The energy profile for the overall process is shown in Scheme 2. Firstly, glycerol adsorbs on the $SrTiO_3$ perovskite surface interacting with the Lewis acid and Brönsted basic sites of the perovskite surface. It is reported that glycerol forms a multidentate surface species of alkoxide species on metal oxides (Copeland et al., 2013b). In the case of $SrTiO_3$ perovskite, its surface Lewis acid sites interact with the hydroxyl groups of C_1 and C_3 from adsorbed glycerol (AG). In addition, it must be mentioned that the basic sites (oxygen atoms) of the $SrTiO_3$ perovskite surface participate with an additional surface interaction now via hydrogen bond from the hydroxyl hydrogen of C_2 and the hydrogen of the C_2 of adsorbed glycerol. The result of this interaction between perovskite surface and AG is the formation of dihydroxyacetone, through TS-1 transition state with an activation barrier of 23.8 kcal/mol (Scheme 2), along with the generation of Brönsted acid sites on the surface.

Then, the reaction continues with the protonation of the primary hydroxyl group and the carbonyl oxygen of dihydroxyacetone by the formed Brönsted acid sites. The protonation of the primary hydroxyl group of dihydroxyacetone induces some weakening of the C-O bond favoring the formation of water. It is well-known that due to the fact the hydroxyl group (-OH) is a poor leaving group, the presence of Brönsted acid sites may often assist the protonation of hydroxyl group of the primary carbon of alcohols (García-Sancho et al., 2018). The result of this step is the formation of 2,3-enol and the elimination of water. It must be also emphasized that HA would be formed rather than 3-hydroxypropanal or acrolein if the primary hydroxyl group is abstracted in the first

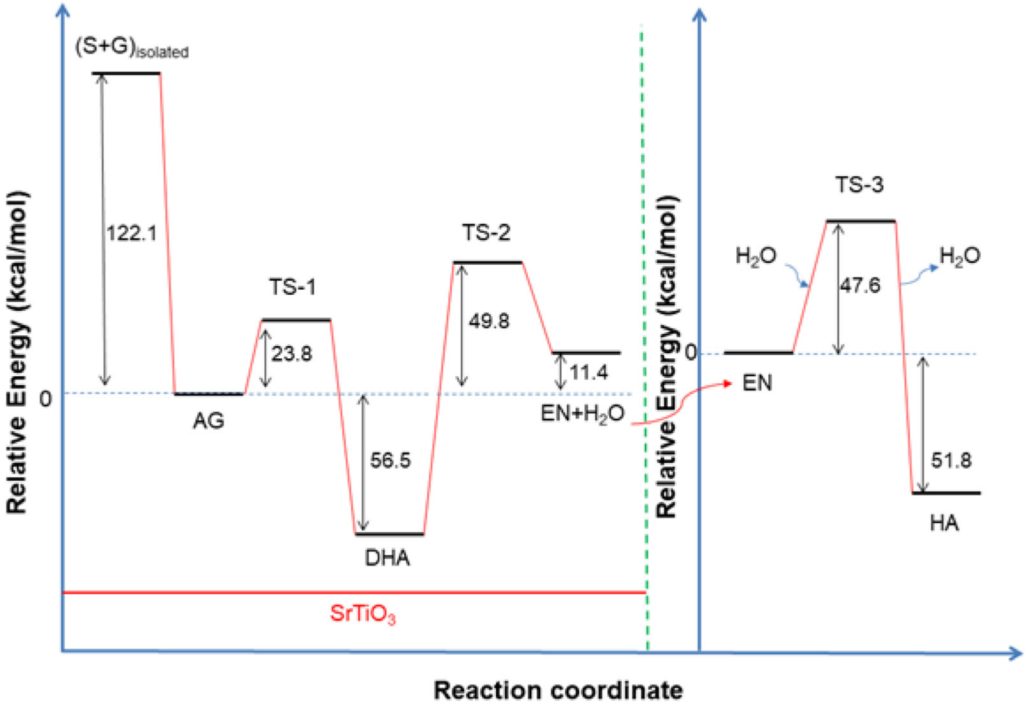

Scheme 2. Potential energy profile along the reaction pathway of transformation of glycerol into hydroxyacetone. Left: reactions of the adsorbed species on the Ti-O terminated surface of $SrTiO_3$. Right: reaction of desorbed species to form HA.

dehydration. It is believed that for this step, Lewis acid sites are more efficient to produce hydroxyacetone instead of acrolein (Alhanash et al., 2010).

It is observed that the limiting rate stage is that corresponding to the formation of 2,3-enol via the occurrence of the transition state TS-2. The respectively calculated activation barrier is 106.3 kcal/mol. This high-value account for the cleavage of the C-O hydroxyl bond to form 2,3-enol which was also revealed to be a rate-determining step of glycerol hydrogenolysis in previous studies (Huang et al., 2008; ten Dam and Hanefeld, 2011). Thus, 2,3-enol is desorbed from the perovskite surface suffering finally tautomerization to generate HA and water elimination. This is indeed the final step for the formation of hydroxyacetone. The activation barrier of this step is 47.6 kcal/mol.

3.7. Proposed mechanism

The proposed mechanism for the overall process is shown in Scheme 3. The first is the adsorption process of the glycerol molecule on the surface of the $SrTiO_3$ perovskite formed by the surface of the Ti-O bonds. In this adsorption in a non-dissociative way, it can be seen the interplay between multiple species through a set of acid-base sites. In this case, the interaction of the Lewis basic sites present in the terminal oxygen atoms of glycerol with a pair of titanium atoms is generated to be adsorbed on the surface. Later, the basic sites of a pair of superficial oxygen atoms of the perovskite abstract two hydrogen atoms from glycerol; one that is directly attached to the secondary carbon and the other is forming part of the secondary hydroxyl group. Both oxygens of the perovskite surface behave as Brönsted basic sites in a concerted mechanism generating a transition state with an activation barrier of 23.8 kcal/mol that results in the formation of two protonated surface oxygens and dihydroxyacetone. The next step is described by the nucleophilic attack of two oxygen atoms of the dihydroxyacetone formed towards the superficial Brönsted acid sites; that is, the concerted and synchronous mechanism for the abstraction of hydrogens by the carbonyl oxygen and by one of the hydroxylic oxygens, eliminating a water molecule and forming 2,3-enol, whose transition state presented a calculated activation barrier of 106.3 kcal/mol. The 2,3-enol is then desorbed from the surface and is prone to interact with water, which is responsible for easing (or mediating) a keto-enolic tautomerism equilibrium to produce hydroxyacetone, with an activation barrier of the state of transition of 47.6 kcal/mol.

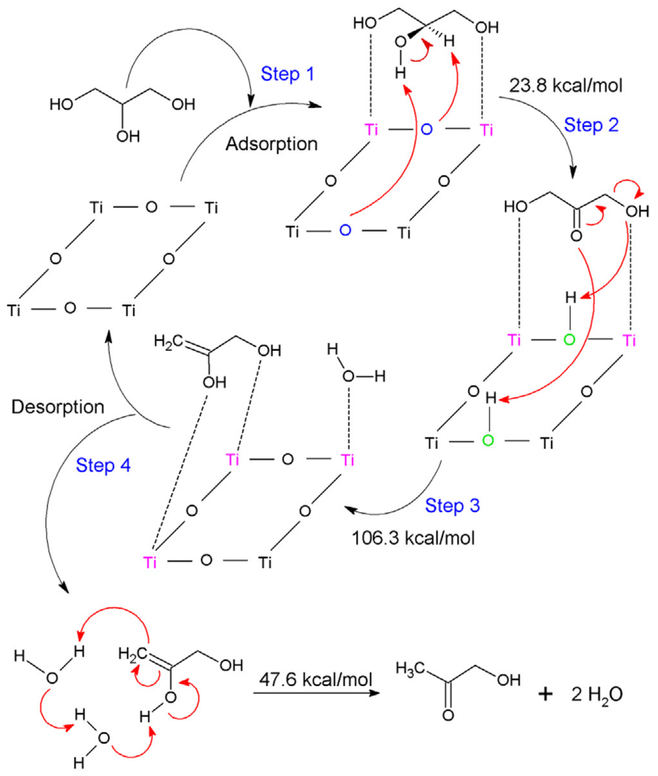

Scheme 3. Proposed catalytic cycle for the conversion of glycerol to HA over $SrTiO_3$ perovskite. The Lewis acid sites represented by the titanium atoms are in color pink, in color blue are the Brönsted basic sites and in green the Brönsted acid sites.

4. Conclusions

The adsorption of glycerol on the Ti-O terminated surface of $SrTiO_3$ occurs in a non-dissociative or molecularly adsorbed way (Lewis-bound species) as expected for Lewis sites, represented by the titanium atoms of the surface. The conversion of glycerol into hydroxyacetone over $SrTiO_3$ perovskite includes the following succession of events: (1) the adsorption of glycerol on the surface of the perovskite; (2) the formation of dihydroxyacetone via the occurrence of the transition state TS-1 showing an activation barrier of 23.8 kcal/mol; (3) formation of 2,3-enol by the respective water elimination in the dihydroxyacetone through the transition state TS-2, having an activation barrier of 106.3 kcal/mol, which results to be the rate-limiting stage; and (4) surface desorption of 2,3-enol with its subsequent keto-enol tautomerism to form the final product hydroxyacetone. The reaction is triggered by the proton transference from both the C_2-hydroxyl group and the C_2 atom toward the Brönsted basic site of the surface, oxygen atoms, to form dihydroxyacetone and to create Brönsted acid sites on the surface. Afterward, these acid sites induce the protonation of both the carbonyl carbon and the terminal hydroxyl group to form 2,3-enol. Then 2,3-enol is desorbed, to finally tautomerize to produce HA. The activation barrier for this last stage is 47.6 kcal/mol. The results stress the dual behavior of the oxygen atoms in the surface, acting firstly as Brönsted base during the formation of dihydroxyacetone, and later as Brönsted acid during the formation of 2,3-enol. In closing, it is also important to reemphasize that the reaction pathway proceeds with the participation of Lewis acid sites represented by the titanium atoms; and Brönsted basic/acid sites represented by the oxygen atoms on the surface. At the end of the catalytic cycle, Brönsted acidic sites are regenerated back to the initial basic surface oxygen atoms of the perovskite surface.

CRediT authorship contribution statement

Ignacio Lizana: Methodology, Validation, Formal analysis, Writing - review & editing. **Julio Colmenares-Zerpa:** Writing - review & editing, Formal analysis. **Gina Pecchi:** Writing - review & editing, Project administration, Funding acquisition. **R.J. Chimentão:** Conceptualization, Writing - review & editing, Formal analysis. **Eduardo J. Delgado:** Writing – original draft, Conceptualization, Validation, Formal analysis, Supervision.

Declaration of Competing Interest

The authors declare that they have no known competing financial interests or personal relationships that could have appeared to influence the work reported in this paper.

Acknowledgements

The authors gratefully acknowledge the financial support from the Chilean National Fund for Science and Technology, Fondecyt

(No 1180243, 1210142); ANID Millennium Science Initiative grant NCN17-040; Chilean National Commission for Science and Technology Fellowship (No 21180277, 21201413), and Universidad de Concepción (VRID No 220.022.030-INV, Internationalization Program UCO 1866).

Appendix A. Supplementary data

Supplementary data to this article can be found online at https://doi.org/10.1016/j.jksus.2021.101597.

References

Alhanash, A., Kozhevnikova, E.F., Kozhevnikov, I.V., 2010. Gas-phase dehydration of glycerol to acrolein catalysed by caesium heteropoly salt. Appl. Catal. A 378 (1), 11–18. https://doi.org/10.1016/j.apcata.2010.01.043.

Arandiyan, H.R., Parvari, M., 2009. Studies on mixed metal oxides solid solutions as heterogeneous catalysts Retrieved from Braz. J. Chem. Eng. 26, 63–74 http://www.scielo.br/scielo.php?script=sci_arttext&pid=S0104-66322009000100007&nrm=iso.

Behr, A., 2008. The future of glycerol. New usages for a versatile raw material. By Mario Pagliaro and Michele Rossi. ChemSusChem 1 (7), 653. https://doi.org/10.1002/cssc.200800115.

Bochevarov, A.D., Harder, E., Hughes, T.F., Greenwood, J.R., Braden, D.A., Philipp, D. M., Rinaldo, D., Halls, M.D., Zhang, J., Friesner, R.A., 2013. Jaguar: A high-performance quantum chemistry software program with strengths in life and materials sciences. Int. J. Quantum Chem. 113 (18), 2110–2142. https://doi.org/10.1002/qua.v113.1810.1002/qua.24481.

Callam, C.S., Singer, S.J., Lowary, T.L., Hadad, C.M., 2001. Computational analysis of the potential energy surfaces of glycerol in the gas and aqueous phases: effects of level of theory, basis set, and solvation on strongly intramolecularly hydrogen-bonded systems. J. Am. Chem. Soc. 123 (47), 11743–11754. https://doi.org/10.1021/ja011785r.

Carlotto, S., Natile, M.M., Glisenti, A., Vittadini, A., 2015. Adsorption of small molecules at the cobalt-doped SrTiO3(001) surface: a first-principles investigation. Surf. Sci. 633, 68–76. https://doi.org/10.1016/j.susc.2014.11.025.

Célerier, S., Morisset, S., Batonneau-Gener, I., Belin, T., Younes, K., Batiot-Dupeyrat, C., 2018. Glycerol dehydration to hydroxyacetone in gas phase over copper supported on magnesium oxide (hydroxide) fluoride catalysts. Appl. Catal. A 557, 135–144. https://doi.org/10.1016/j.apcata.2018.03.022.

Chaminand, J., Djakovitch, L.A., Gallezot, P., Marion, P., Pinel, C., Rosier, C., 2004. Glycerol hydrogenolysis on heterogeneous catalysts. Green Chem. 6 (8), 359. https://doi.org/10.1039/b407378a.

Charoenwiangnuea, P., Maihom, T., Kongpracha, P., Sirijaraensre, J., Limtrakul, J., 2016. Adsorption and decarbonylation of furfural over H-ZSM-5 zeolite: a DFT study. RSC Adv. 6 (107), 105888–105894. https://doi.org/10.1039/C6RA24631A.

Chelli, R., Gervasio, F.L., Gellini, C., Procacci, P., Cardini, G., Schettino, V., 2000. Conformational distribution of gas-phase glycerol. J. Phys. Chem. A 104 (47), 11220–11222. https://doi.org/10.1021/jp002677e.

Coma, M., Martinez-Hernandez, E., Abeln, F., Raikova, S., Donnelly, J., Arnot, T.C., Allen, M.J., Hong, D.D., Chuck, C.J., 2017. Organic waste as a sustainable feedstock for platform chemicals. Faraday Discuss. 202, 175–195. https://doi.org/10.1039/C7FD00070G.

Copeland, J.R., Santillan, I.A., Schimming, S.M., Ewbank, J.L., Sievers, C., 2013a. Surface interactions of glycerol with acidic and basic metal oxides. J. Phys. Chem. C 117 (41), 21413–21425. https://doi.org/10.1021/jp4078695.

Copeland, J.R., Shi, X.-R., Sholl, D.S., Sievers, C., 2013b. Surface interactions of C2 and C3 polyols with γ-Al2O3 and the role of coadsorbed water. Langmuir 29 (2), 581–593. https://doi.org/10.1021/la304074x.

Dapsens, P.Y., Mondelli, C., Pérez-Ramírez, J., 2015. Design of Lewis-acid centres in zeolitic matrices for the conversion of renewables. Chem. Soc. Rev. 44 (20), 7025–7043. https://doi.org/10.1039/C5CS00028A.

García-Sancho, C., Cecilia, J.A., Mérida-Robles, J.M., Santamaría González, J., Moreno-Tost, R., Infantes-Molina, A., Maireles-Torres, P., 2018. Effect of the treatment with H3PO4 on the catalytic activity of Nb2O5 supported on Zr-doped mesoporous silica catalyst. Case study: glycerol dehydration. Appl. Catal. B 221, 158–168. https://doi.org/10.1016/j.apcatb.2017.09.016.

Hay, P.J., Wadt, W.R., 1985. Ab initio effective core potentials for molecular calculations. Potentials for the transition metal atoms Sc to Hg. J. Chem. Phys. 82 (1), 270–283. https://doi.org/10.1063/1.448799.

Housaindokht, M.R., Zamand, N., 2015. A DFT study of associative and dissociative chemical adsorption of DMMP onto SnO2(110) surface nano-cluster. Struct. Chem. 26 (1), 87–96. https://doi.org/10.1007/s11224-014-0465-8.

Huang, Z., Cui, F., Kang, H., Chen, J., Zhang, X., Xia, C., 2008. Highly dispersed silica-supported copper nanoparticles prepared by precipitation−Gel method: a simple but efficient and stable catalyst for glycerol hydrogenolysis. Chem. Mater. 20 (15), 5090–5099. https://doi.org/10.1021/cm8006233.

Ketchie, W.C., Murayama, M., Davis, R.J., 2007. Selective oxidation of glycerol over carbon-supported AuPd catalysts. J. Catal. 250 (2), 264–273. https://doi.org/10.1016/j.jcat.2007.06.011.

Kinage, A.K., Upare, P.P., Kasinathan, P., Hwang, Y.K., Chang, J.-S., 2010. Selective conversion of glycerol to acetol over sodium-doped metal oxide catalysts. Catal. Commun. 11 (7), 620–623. https://doi.org/10.1016/j.catcom.2010.01.008.

Kongpatpanich, K., Nanok, T., Boekfa, B., Probst, M., Limtrakul, J., 2011. Structures and reaction mechanisms of glycerol dehydration over H-ZSM-5 zeolite: a density functional theory study. PCCP 13 (14), 6462–6470. https://doi.org/10.1039/C0CP01720E.

Lari, G.M., Mondelli, C., Pérez-Ramírez, J., 2015. Gas-phase oxidation of glycerol to dihydroxyacetone over tailored iron zeolites. ACS Catal. 5 (3), 1453–1461. https://doi.org/10.1021/cs5019056.

Li, X., Zhang, L., Wang, S., Wu, Y., 2020. Recent advances in aqueous-phase catalytic conversions of biomass platform chemicals over heterogeneous catalysts. Front. Chem. 7 (948). https://doi.org/10.3389/fchem.2019.00948.

Lima, C.L., Vasconcelos, S.J.S., Filho, J.M., Neto, B.C., Rocha, M.G.C., Bargiela, P., Oliveira, A.C., 2011. Nanocasted oxides for gas phase glycerol conversion. Appl. Catal. A 399 (1), 50–62. https://doi.org/10.1016/j.apcata.2011.03.036.

Longo, V.M., de Figueiredo, A.T., de Lázaro, S., Gurgel, M.F., Costa, M.G.S., Paiva-Santos, C.O., Varela, J.A., Longo, E., Mastelaro, V.R., DE Vicente, F.S., Hernandes, A. C., Franco, R.W.A., 2008. Structural conditions that leads to photoluminescence emission in SrTiO3: an experimental and theoretical approach. J. Appl. Phys. 104 (2), 023515. https://doi.org/10.1063/1.2956741.

Madura, J.D., Ul-Haq, Z., 2017. Frontier in Computational Chemistry, (Vol. 3):. Bentham Books.

Pecchi, G., Jiliberto, M.G., Buljan, A., Delgado, E.J., 2011. Relation between defects and catalytic activity of calcium doped LaFeO3 perovskite. Solid State Ionics 187 (1), 27–32. https://doi.org/10.1016/j.ssi.2011.02.014.

Polo-Garzon, F., Wu, Z., 2018. Acid–base catalysis over perovskites: a review. J. Mater. Chem. A 6 (7), 2877–2894. https://doi.org/10.1039/C7TA10591F.

Pompeo, F., Santori, G., Nichio, N.N., 2010. Hydrogen and/or syngas from steam reforming of glycerol. Study of platinum catalysts. Int. J. Hydrogen Energy 35 (17), 8912–8920. https://doi.org/10.1016/j.ijhydene.2010.06.011.

Sanchez, Astrid, Velasquez, Mauricio, Batiot-Dupeyrat, Catherine, Espinal, Juan F., Santamaría, Alexander, 2019. Mechanism of glycerol dehydration and dehydrogenation: an experimental and computational correlation. DYNA 86 (208), 126–135.

Sels, B., D'Hondt, E., Jacobs, P., 2007. Catalysis for Renewables: From feed Stock to Energy Production. Wiley-VCH, Weinhem.

Shen, Y., Zhang, S., Li, H., Ren, Y., Liu, H., 2010. Efficient synthesis of lactic acid by aerobic oxidation of glycerol on Au–Pt/TiO2 Catalysts. Chem. A Eur. J. 16 (25), 7368–7371. https://doi.org/10.1002/chem.201000740.

Smith, M.B., March, J., 2007. March's Advanced Organic Chemistry Reactions, Mechanisms, and Structure. John Wiley & Sons.

Stošić, Dušan, Bennici, Simona, Sirotin, Sergey, Stelmachowski, Pawel, Couturier, Jean-Luc, Dubois, Jean-Luc, Travert, Arnaud, Auroux, Aline, 2014. Examination of acid–base properties of solid catalysts for gas phase dehydration of glycerol: FTIR and adsorption microcalorimetry studies. Catal. Today 226, 167–175. https://doi.org/10.1016/j.cattod.2013.11.047.

Suprun, W., Lutecki, M., Gläser, R., Papp, H., 2011. Catalytic activity of bifunctional transition metal oxide containing phosphated alumina catalysts in the dehydration of glycerol. J. Mol. Catal. A Chem. 342–343, 91–100. https://doi.org/10.1016/j.molcata.2011.04.020.

ten Dam, J., Hanefeld, U., 2011. Renewable chemicals: dehydroxylation of glycerol and polyols. ChemSusChem 4 (8), 1017–1034. https://doi.org/10.1002/cssc.201100162.

Wade, L.G., 2006. Organic Chemistry. Pearson Education.

Wadt, W.R., Hay, P.J., 1985. Ab initio effective core potentials for molecular calculations. Potentials for main group elements Na to Bi. J. Chem. Phys. 82 (1), 284–298. https://doi.org/10.1063/1.448800.

Yang, M.-M., Bao, X.-H., Li, W.-X., 2007. First principle study of ethanol adsorption and formation of hydrogen bond on Rh(111) surface. J. Phys. Chem. C 111 (20), 7403–7410. https://doi.org/10.1021/jp0686184.

Yun, Y.S., Kim, T.Y., Yun, D., Lee, K.R., Han, J.W., Yi, J., 2017. Understanding the reaction mechanism of glycerol hydrogenolysis over a CuCr2O4 catalyst. ChemSusChem 10 (2), 442–454. https://doi.org/10.1002/cssc.201601269.